Automatic Events Extraction in Pre-stack Seismic Data Based on Edge Detection in Slant-stacked Peak Amplitude Profiles

Jing Zhao[1], Jinchang Ren[2,5], Jinghuai Gao[3], Julius Tschanner[2], Paul Murray[2], Daxing Wang[4]

[1] School of Earth Science and Engineering, Xi'an Shiyou University, Xi'an, China.

[2] Department of Electronic and Electrical Engineering, University of Strathclyde, Glasgow, UK

[3] Institute of Wave and Information, School of Electronic and Information Engineering, Xi'an Jiaotong University, Xi'an, China.

[4] Research Institute of E & D, Changqing Oil-Field Company of CNPC, Xi'an, China

[5] College of Electrical and Power Engineering, Taiyuan University of Technology, Taiyuan, China

***Abstract*— Events picking is one of the fundamental tasks in interpreting seismic data. To extract the correct travel-time of reflected waves, picking events in a wide range of source-receiver offsets is needed. Compared to post-stack seismic data, pre-stack seismic data has an accurate horizon and abundant travel-time, amplitude, and frequency while the waveform of post-stack data is damaged by normal move-out (NMO) applications. In this paper, we focus on automatic event extraction from pre-stack reflection seismic data. With the deep development of oil-gas exploration, the difficulty of petroleum exploration is being increased. Auto recognition and picking of seismic horizon is presented as the basis for oil-gas detection. There is a correspondence between the real geology horizon and events of seismic profiles. As a result, firstly, recognizing and tracing continuous events from real seismic records are needed to acquire significant horizon locations. Picking events is in this context the recognition and tracing of waves reflected from the same interfaces according to kinematics and dynamic characteristics of seismic waves. Current extraction algorithms are well able to trace these events of the seismic profile and are undergoing great development and utilization. In this paper, a method is proposed to pick travel-time and local continuous events based on edges obtained by slant-stacked peak amplitude section (SSPA). How to calculate the SSPA section is discussed in detail. The new method can improve the efficiency and accuracy without windowing and manual picking of seed points. The event curves obtained from both the synthetic layered model and field record have validated the high accuracy and efficiency of the proposed methodology.**

Index Terms—Automatic event extraction; pre-stack reflection data; ray tracing; Radon transformation.

1. Introduction

Automatic events extraction is the process of recognizing and tracing reflection waves from the horizon according to kinematics and dynamic characteristics of seismic waves. In the field of seismic exploration, it is very important to recognize and trace the stratigraphic horizon. The real geology horizon generally corresponds to events at the seismic profile, hence tracing the events of the real seismic record is a key factor in acquiring the correct horizon locations (Zhao, 2018). The events can be used to analyze the seismic wave propagation on the subsurface medium and to derive the geologic structure and the expanding characteristic of stratum.

Events can be acquired by connecting the reflection waves which have the same phases. In traditional methods, the interpreter recognizes and traces seismic events by comparing the phases of one or more maxima of waves in each trace of the seismic records. As manual tracing of events was of poor accuracy, time-consuming, and subjectivity sensitive (Wang and Gao, 2012) , automatic events picking technologies such as cross-correlation (Ding et al., 2012) and neural networks (Lu and Mou, 1998) were proposed since the early 1980s. Recently, there are two categories of auto picking methods widely used, i.e. character tracing and correlation tracing (Zhen, 2013). However, both these methods have difficulties picking events continuously and have a low signal-to-noise-ratio (SNR).

Several edge detection based methods were recently proposed by Li (Li, 2014), Wang (Wang and Sun, 2016), Xiang (Xiang et al., 2017), Karbalaali (Karbalaali et al., 2017), Bondar (Bondar, 1992), Li (Li et al., 2007), Xiong (Xiong et al., 2009) and Yang (Yang and Cheney, 2011), where image processing on gray scale images of seismic gather and edge detection are used to detect events. The envelope of the gray mutation areas is interpreted as events after some post-processing, e.g. morphological thinning. The results however are ambiguous, have low resolution and are easily affected by noise.

Different from the linear detection technology mentioned above, Faraklioti (Faraklioti, 2004) proposed an automatic horizon extraction method from 3-D seismic data based on surface detection. This method however has a higher complexity and computational cost. In McCormack (McCormack, 1993) and Glinsky (Glinsky, 2001), neural networks are employed to use known events as the standard samples to train the network. The weight values of neurons are modified step by step using the error back-propagation algorithm. The network is able to process new data when the algorithm can find the optimal weight distribution. Finding sufficient training samples for the network has however proven difficult, also the trained network could be affected by the new samples. Additionally, the training process is very time consuming due to the large amount of iterations.

In both the adaptive coherent picking technique proposed by Spagnolini (Spagnolini, 1991) and the high order cumulants method proposed by Tugnait (Tugnait, 1991) and Feng (Feng et al., 2011), similar characteristics of waveforms of the events among different traces are used. Xu (Xu et al., 1990) introduced a chain match method in which a chain is constructed by crest and

several features is used to represent each trace of the wave forms. Bian (Bian, 1991) manually picked some control points (seed points) of seismic events followed by interpolation, where they filtered out the outliers with high frequencies produced during the interpolation process. This method has difficulties in achieving automatic events picking because of the manual picking of the seed points. Zhou (Zhou and Hu, 1991) proposed a fitting method which interprets the events as dynamic curves. The curves are described by generalized time series and are fitted by models such as AR (Auto Regressive) model. An appropriate model and the arrival-time of waves are difficult to determine, which will affect the results of events fitting.

Probabilistic modelling is also one main stream of approaches in auto event picking. Woodham (Woodham, 1995) proposed a probabilistic data association algorithm which models the horizons to be extracted as first order ordinary differential equations. This method traces the horizon information gradually according to the results of the data association achieved by calculating the posterior probability of each observed vector. In Li (Li, et al., 2005) and Zhao (Zhao et al., 2006), a chaos oscillator detection method was used to detect weak events according to a modified Duffing equation. This method scans the events to construct equal time interval series according to an assumed pair of time and velocity. Finally, the series is sent to the chaos oscillator system and the extraction results are acquired according to the difference of phase. This method can extract events even in the case of extremely low *SNR*. This method however requires to search the pair of time and velocity and to solve the differential equations of the chaos oscillator system, which resulted in inefficiencies. Most of the existing methods do not incorporate the motion law of seismic waves, have a high computation complexity and have difficulties to automatically extract events from noisy data.

In this paper, an automatic travel-time and continuous events picking method at large offsets of seismic data is presented that utilizes edge detection based on peak amplitude profiles. Events are picked continuously with a large offset to obtain correct travel times of the reflections. Compared to other state of the art methods, this method has the advantage of being able to process data with a high *SNR* and is easy to implement. It overcomes the difficulty of existing approaches, manually or automatically, when picking continuous events in large offset areas.

2. **Theory**

Travel-time is an important parameter for attenuation and velocity tomography of seismic data. To determine the travel-time of a reflection wave, events are required to be picked in a wide range of offsets. Events picking is one of the basic steps for seismic interpretation. However, it is often difficult to successively pick continuum events in large offsets due to noise in the recorded data. Post-stack reflection data has high signal to noise ratio (*SNR*), but part of the amplitude and frequency information are damaged after the stretching and the stacking of normal move-out (*NMO*). The damage result in some subtle features being difficult to recognize. Compared to the post-stack reflection data, the pre-stack seismic reflection data has low *SNR*, but it is not affected by *NMO*, and have exact layer information, abundant frequency and travel-time information. The minute stratum features such as the

variation of the waveform at the thin interbed series can be observed from the pre-stack data. Based on the abundance of amplitude and frequency information, it is important to study the events extraction method for pre-stack seismic record.

In this paper, an edge detection analysis based on SSPA profiles is proposed for events picking in seismic data. Slant-stack is carried out because it serves as a filter and can reduce the noise. After Fourier transform and Hilbert transform, the real signal can be translated to complex signal, and the instantaneous amplitude (IA) can be obtained from the complex signal. The IA can reflect signal energy at any given time and the low frequency information. The IA section can filter some high frequency noise in a way, but its anti-noise capacity is weak. Studies on Slant-stack (namely, τ-p transform) do find a strong anti-noise property when stacking the amplitude along the gradient. We define the peak amplitude section after slant stacking as the SSPA profile. The SSPA profile is obtained by implying slant-stack transformation on the IA section but not the original seismic record, this is because the IA section has better quality than the seismic record. SSPA profile has better SNR than the IA section and the original seismic data. This is because that the noise is counteracted when slant stacking. Afterwards, the edge detection profile is calculated based on the SSPA profile. The new method can also apply to pose-stack seismic data.

The IA section is calculated as follow (Barnes, 1991, 1993):

$$a(t)=\left\| s(t)+i\cdot H\left[s(t) \right] \right\| \tag{1}$$

where $a(t)$ is instantaneous amplitude, $s(t)$ the trace of seismic data and $H\left[s(t) \right]=\mathrm{Im}[C_g^{-1}\int_{-\infty}^{+\infty}S(b,a)s^{-1}ds$ the Hilbert signal obtained from wavelet transformation (*WT*). $S(b,a)$ is the *WT* of the seismic data. The *WT* of $s(t)$ for the wavelet function $g(t)$ is defined as：

$$S(b,a)=\frac{1}{a}\int_{-\infty}^{+\infty}s(t)\bar{g}\left(\frac{t-b}{a} \right)dt \tag{2}$$

where, $t,b\in\mathbf{R}$， $a>0$, $g(t)\in L^1(\mathbf{R},dt)\bigcap L^2(\mathbf{R},dt)$ is a wavelet function, $\bar{g}(t)$ is the complex conjugate of $g(t)$, L^1 and L^2 are each absolutely and quadratic integrable spaces. C_g is the admissible condition of the wavelet translation.

Slant-stack is carried out using the local Radon transformation. It is applied on the IA section to stack several traces nearby the reference trace. In this way, a super-gather can be constructed to increase the SNR. The Linear Radon transformation is also called τ-*p* transformation. The integral path is linear. The τ-*p* transform is used to acquire the parameters of the rays. In the frequency domain, the discrete linear Radon transformation is defined by (Shen et al., 2000):

$$M(f,p)=\sum_{m=1}^{nx}A(f,x_m)e^{j2\pi fpx_m} \tag{3}$$

where $M(f,p)=\int m(\tau,p)e^{-j2\pi f\tau}d\tau$, $m(\tau,p)$ is the Radon transformation in the time domain . $A(f,x_m)=\int a(t,x_m)e^{-j2\pi ft}dt$ is the Fourier transform of $a(t, x_m)$ and x_m is the referential trace. The IA data is zero-padded before applying the Radon transformation with a length of three times the original signal in the time domain to increase the frequency resolution.

The local Radon transformation of the IA section is obtained by the following procedure:

1) Choose a reference trace from the IA section.

2) For a certain sample time pot τ_i, add up the amplitude of the several traces nearby the reference trace in n_p different gradient values p_j ($j=1,2,\cdots,n_p$) with a step Δp (shown in Fig. 1).

3) Calculate the sum of IA under different directions and record the results on the corresponding positions in the τ-p domain.

4) When the chosen gradient for adding up is close or equal to the gradient of the event of the observed record, the added value is maximum in τ-p domain.

5) Pick the maximal value of the slant stack amplitude data, which is called the SSPA, and record it on the corresponding position in t-x domain.

By applying this procedure, a super-gather section is constructed, which is called the SSPA section to improve the *SNR*. Compared to the IA section, the events of the SSPA section are much clearer and have less interference. This is because the noise is reduced further when several data traces of the neighborhood are added up in the gradient.

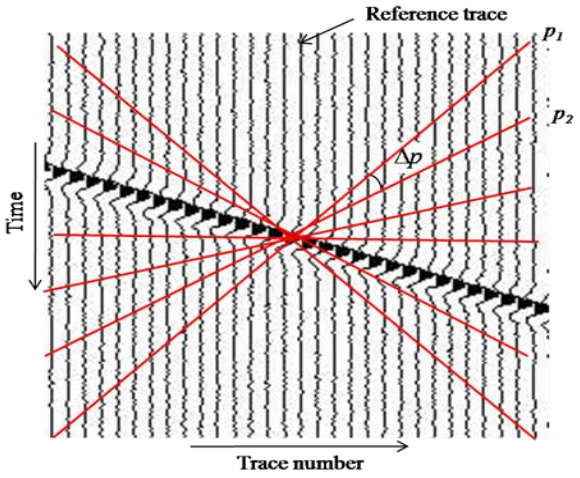

Fig. 1 Radon transform diagram

Edge detection can be used to detect structural variations and relevant properties in image data and can therefore be used to reduce the data amount. It is an important research field in feature extraction. Edges are defined as small areas of the image where the gray value or intensity is not continuous or produces mutations. The elements of the edge form the border in the images. Depending on the image acquisition process of the source data, edge detection may vary in quality. Usually, pre-processing steps,

such as gradient, that enhance the image edges are carried out to achieve the best recognition results. In the field of digital imaging, seismic profile can be considered as a 2D image and the reflection events as lines within these images.

The gradient operator is used to extract edges. Assume the gray degree field is $f(x, y)$, the corresponding gradient value is defined by:

$$gradf(x, y) = \left[\frac{\partial f}{\partial x}, \frac{\partial f}{\partial y} \right]^T \tag{4}$$

The absolute value of equation (4) is defined by:

$$\left| gradf(x, y) \right| = \sqrt{\left(\frac{\partial f}{\partial x} \right)^2 + \left(\frac{\partial f}{\partial y} \right)^2} \tag{5}$$

In the discrete case, equation (5) can be replaced by the differential form:

$$\Delta x\, f(x, y) = f(x, y) - f(x-1, y) \tag{6}$$

$$\Delta y\, f(x, y) = f(x, y) - f(x, y-1) \tag{7}$$

Specifically, the Sobel, Prewitt and Canny operators are used as the gradient operator:

(1) **The Sobel operator** is defined as following:

$$s(i, j) = \sqrt{f_x^2 + f_y^2}\text{, equivalent to, } s(i, j) = max\left(\left| f_x \right|, \left| f_y \right| \right) \tag{8}$$

$$f_x = \left(f(i-1, j-1) + 2f(i-1, j) + f(i-1, j+1) \right) - \left(f(i+1, j-1) + 2f(i+1, j) + f(i+1, j+1) \right) \tag{9}$$

$$f_y = \left(f(i-1, j-1) + 2f(i, j-1) + f(i+1, j-1) \right) - \left(f(i-1, j+1) + 2f(i, j+1) + f(i+1, j+1) \right) \tag{10}$$

Given the appropriate threshold β, if the edge strength $S(i, j) > \beta$, the point (i, j) is determined as an edge point. For the threshold β, the smaller the value is, the more detailed edges it can detect. Therefore, appropriate threshold needs be chosen for proper detection of image edges. Here there are two defining methods: one is self-defining, for example, we can choose 0.8 times of the maximum gray value as the threshold; the other is adaptive method, where the threshold can be determined by some constraint conditions.

(2) **The Prewitt operator** is defined as following:

$$P(i, j) = \sqrt{f_x^2 + f_y^2}\text{, equivalent to, } p(i, j) = max\left(\left| f_x \right|, \left| f_y \right| \right) \tag{11}$$

Edge detection formulas are defined as:

$$\begin{aligned} \Delta x f(i, j) &= f(i-1, j-1) + f(i-1, j) + f(i-1, j) + (f(i+1, j-1) - \left[f(i+1, j-1) + f(i+1, j) + f(i+1, j+1) \right] \\ \Delta y f(i, j) &= f(i-1, j-1) + f(i, j-1) + f(i+1, j-1) + (f(i+1, j-1) - \left[f(i-1, j+1) + f(i, j+1) + f(i+1, j+1) \right] \end{aligned} \tag{12}$$

Given the appropriate threshold w, if $P(i, j) > w$, the processed point (i, j) is considered as the edge point.

(3) The workflow of **the Canny operator** for edge detection is given as follows:

a) Smooth the image using a Gaussian filter with optimal parameters neighbourhood size and standard deviation. The image $S(x, y)$ is obtained by the convolution of the Gaussian filter $G(x, y)$ with the image $f(x, y)$.

b) To obtain the normal vector and edge strength $A(i, j)$ at the point (i, j) of the image $f(x, y)$, the direction and amplitude of the gradient of the image are calculated using the finite difference method of the first-order partial derivative.

c) Inhibiting the non-maximum of the amplitude of the image gradient: We use the non-maximum inhibition method rather than edge strength $A(i, j)$ to make sure whether the image $f(x, y)$ is the edge at the point (i, j). If the edge strength value $A(i, j)$ at the pixel (i, j) is less than the strength of the two neighborhood pixels in gradient direction, this pixel is not the edge. In this situation, the strength $A(i, j)$ is set as zero.

The flowchart for edge detection based auto events picking is summarized in Fig. 2:

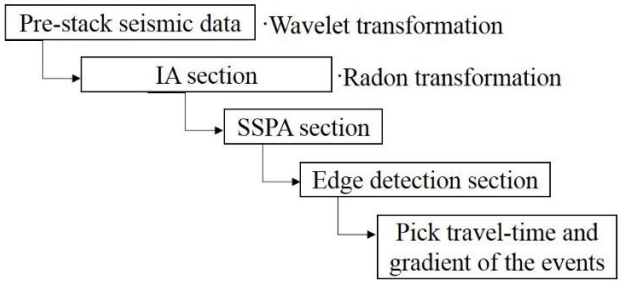

Fig.2 Flowchart of edge detection based auto events picking

3. Experimental results and discussions

3.1 Data set 1: Synthetic pre-stack CMP data

The proposed auto events picking method is validated by using a synthetic pre-stack model. The pre-stack CMP data is synthetized by ray trace method based on the Fermat principle. We assume that the source wavelet can be approximated by the constant phase wavelet with four parameters:

$$u(0,t) = A\left(\frac{\delta^2}{\pi}\right)^{1/4} \exp\left[i(\sigma t + \varphi) - \frac{(\delta t)^2}{2}\right] \tag{13}$$

where A and φ are the amplitude and phase respectively, σ is modulation angular frequency, δ is energy absorption factor. The Fourier transform of formula (13) is:

$$U(0,\omega) = A\left(\frac{4\pi}{\delta^2}\right)^{1/4} \exp\left[-\frac{(\omega-\sigma)^2}{2\delta^2} + i\varphi\right] \tag{14}$$

When the seismic source propagate at the depth of Δz, the frequency domain expression of the wavelet is:

$$U(\Delta z,\omega) = G(\Delta z)\,\mathrm{U}(0,\omega)\exp\left[-\frac{i\omega\Delta z}{c(\omega)} - \frac{\omega\Delta z}{2c(\omega)Q}\right] \tag{15}$$

where, $i=\sqrt{-1}$, ω is the angular frequency, Δz is the propagation distance, $G(\Delta z)$ is the factor which is independent of frequency and absorption, $c(\omega)$ is phase velocity.

The seismic record has 49 traces. The length is 1600ms, and the sample interval is 1ms. Fig. 3 shows that the synthetic data has 5 reflected events. Fig.4(a) is the IA section of the synthetic record. Fig.4(b) is the SSPA section based on the IA section. Fig.4 show that the locations of the events on the two sections are correct, but the SSPA centralizes the effective information which makes the edge detection easier.

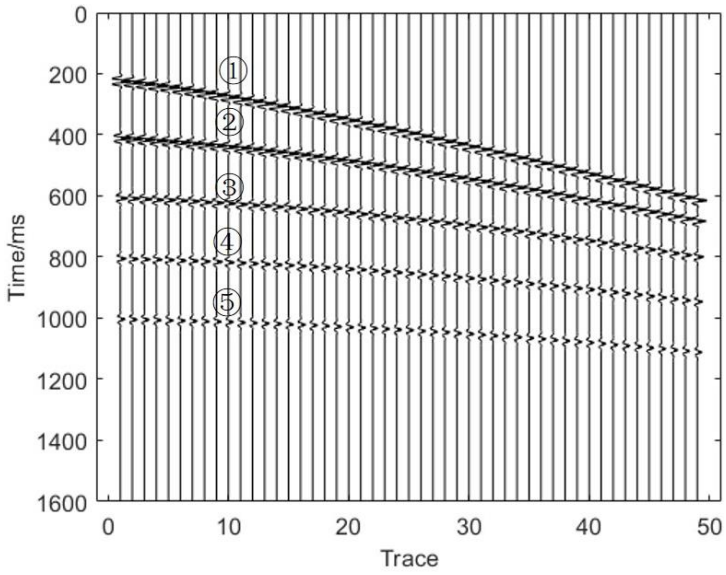

Fig.3 Synthetic seismic section

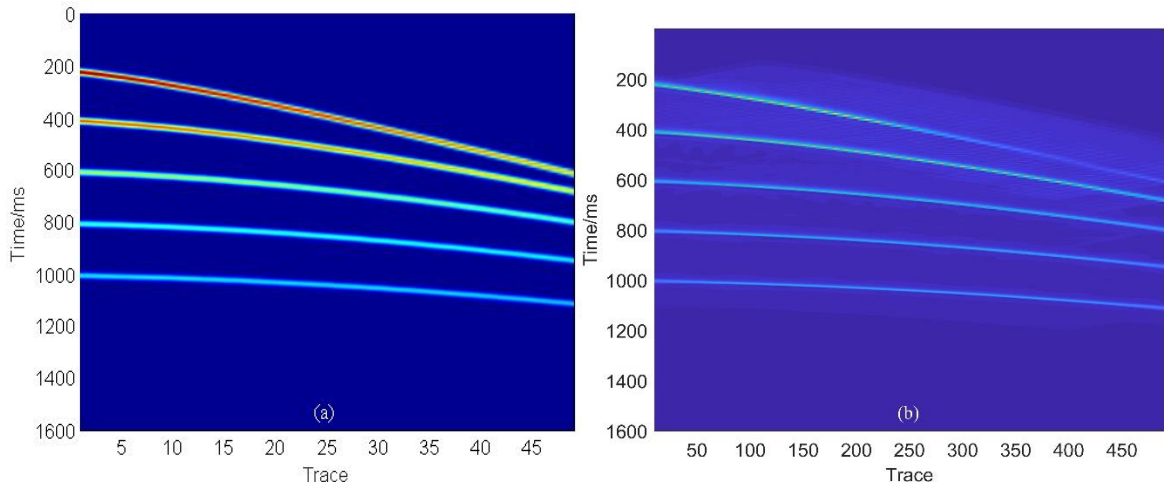

Fig.4 (a) The IA section of the synthetic record; (b) The SSPA section based on the IA section

Edge detection is a very important step in our method. This paper compares the merits of three operators used for edge detection and choses one optimal operator to pick events based on real seismic record. For the Sobel operator and Prewitt operator, the results are illustrated in Fig. 5. In the Prewitt operator, edges are detected from a gray scale image of the seismic section in the eight directions of east, west, south, north, southeast, northeast, southwest, and northwest, and the maximal response from the 8 directions is selected as the edge response.

As can be seen in Fig. 5(a), for the Sobel operator, the results of edge detection can recognize events ① and ②, but the recognition result for events ③, ④ and ⑤ are inaccurate and discontinuous, and there are glitch in the last three events. Fig. 5(b) shows that, for the Prewitt operator, the positions of the five events are consistent with the original image which is the same with the Sobel operator, but they are all discontinuous, where large offset can be found in the five events. To extract smooth and continuous events is aimed to be obtained, so these two operators are not very well.

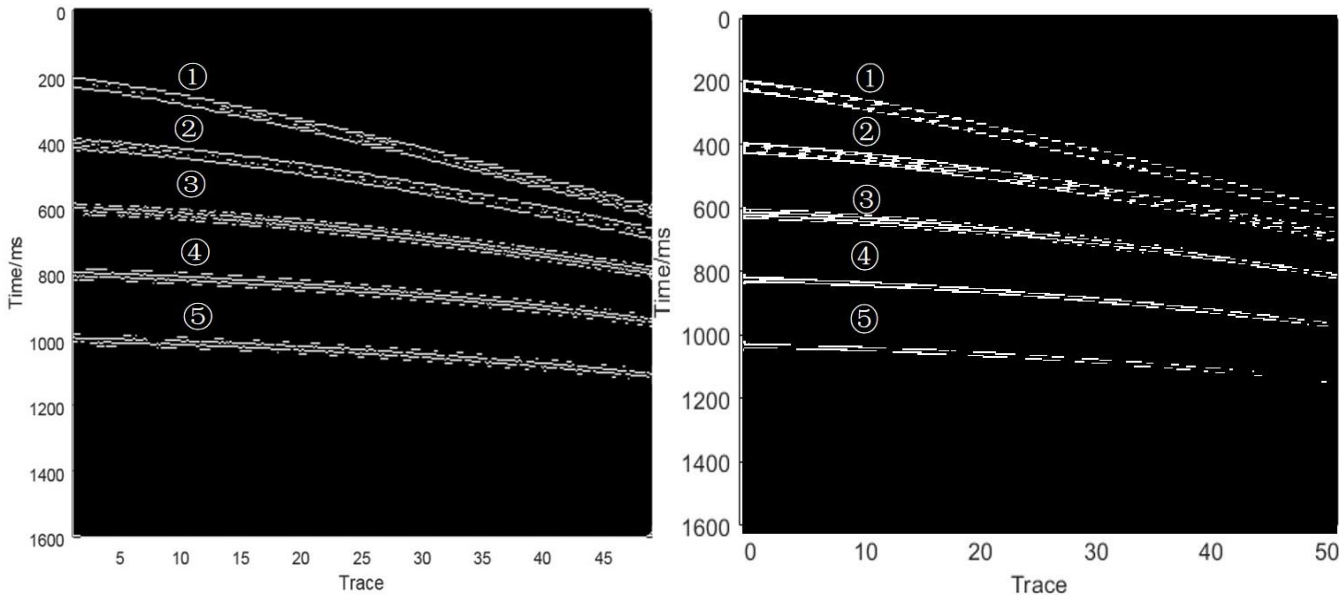

(a) (b)

Fig. 5 Results of edge detection using the Sobel operator (a) and Prewitt operator (b).

The results of edge detection from the Canny operator is given in Fig. 6(a), in which the information of image edges can be effectively extracted and preserved, even for tiny edges within the image. In summary, the result using the Sobel operator is better than that of the Prewitt operator, yet the result from the Canny operator is the best among these three operators. When using the Canny operator, the five events are continuous and accurate, this is because that the Canny operator can maximally preserve the edge information of the image while detecting tiny edges. This means it can extract more subtle seismic events. For complex seismic data however, the Canny operator will keep more noise and affect the result of events extraction.

Using the aforementioned edge operators, the mutation edge of the gray scale image can be detected. The results however are the edges of the events and can't be considered as the result of auto extracted events. If the value of the grayscale image of the seismic section between the two edges is larger than a certain value, the area between the edges is considered as an event. As the results from the Canny operator are the best, the gray value is examined to extract the events by comparing it against a threshold. Because the result of the edge detection is logical data, namely the valid signal is 1 and the background is 0, the threshold can be decided as 0.5. The results of picked events ①~⑤ are also shown in Fig. 6(b), which is highlighted as bold solid line. As can be seen, the events have been successfully extracted from the edge detection results using the Canny operator.

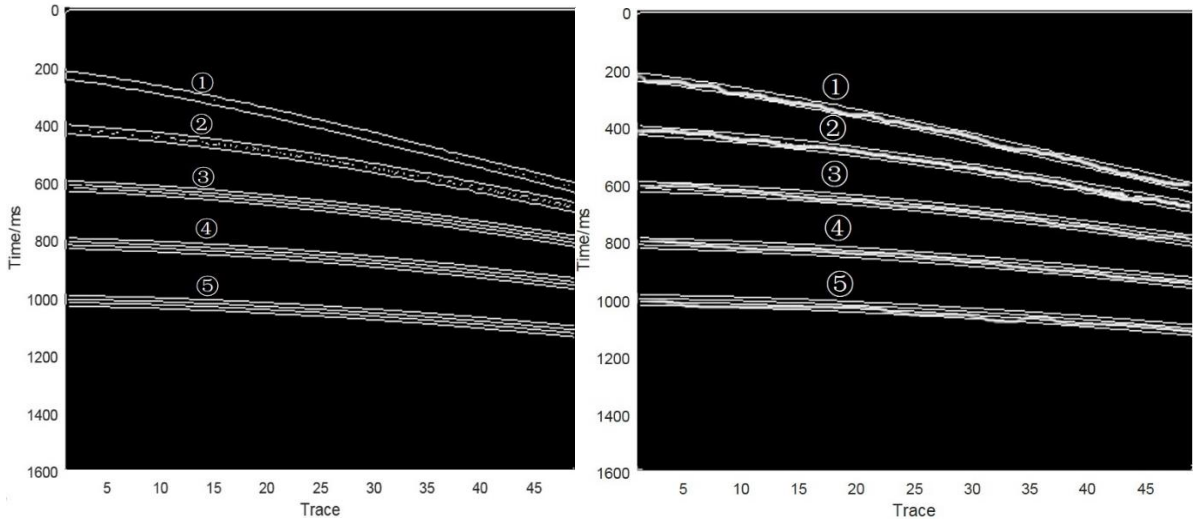

(a) (b)

Fig. 6 Results from the Canny operator for edge detection (a) and auto event picking (b).

3.2 Data set 2: Synthetic pre-stack CMP data with Gaussian noise

To tackle the noise within the real seismic records, it is necessary to analyze the anti-noise capability of the proposed method. Noisy signals with 5 layers are illustrated in Fig.7, where the Gaussian white noise is used with a *SNR* (signal noise ratio) of 5. Fig. 8(a) is the IA section of the synthetic record, which shows that there is noise (for example, the noise in the ellipse) in the background. Fig. 8(b) is the SSPA section based on the IA section, which shows that the background of the SSPA section is very clear. This result confirms our conclusion that the SSPA section has better anti-noise immunity than the IA section. Fig. 9(a) is the results of edge detection, we can see that the five events can be detected and each event is detected as the lower and upper boundaries. Fig. 9(b) shows the extracted events by examining the gray values based on the lower and upper boundaries. By comparing Fig.7 and 9(b), the locations of the events of the two records are consistent, and the extracted events are clear and continuous. The experiment result show that the proposed method has strong ability to resist random noise.

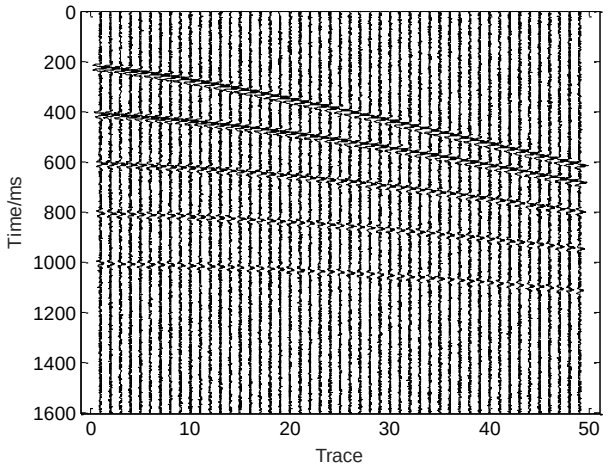

Fig. 7 Synthetic seismic section with Gaussian white noise

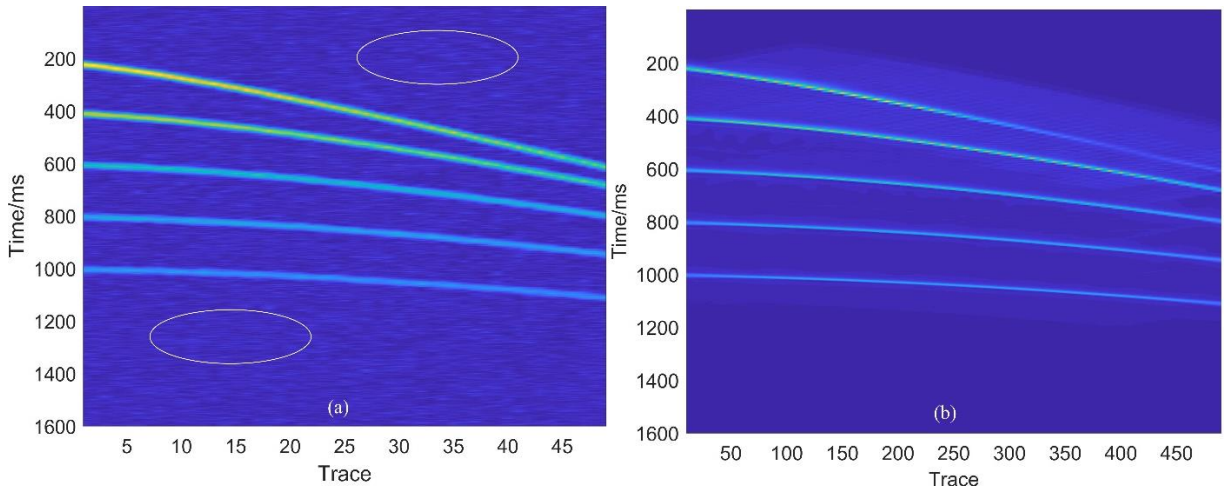

Fig. 8 The IA section of the synthetic record (a, left) and the SSPA section based on the IA section when the SNR is 5 (b, right).

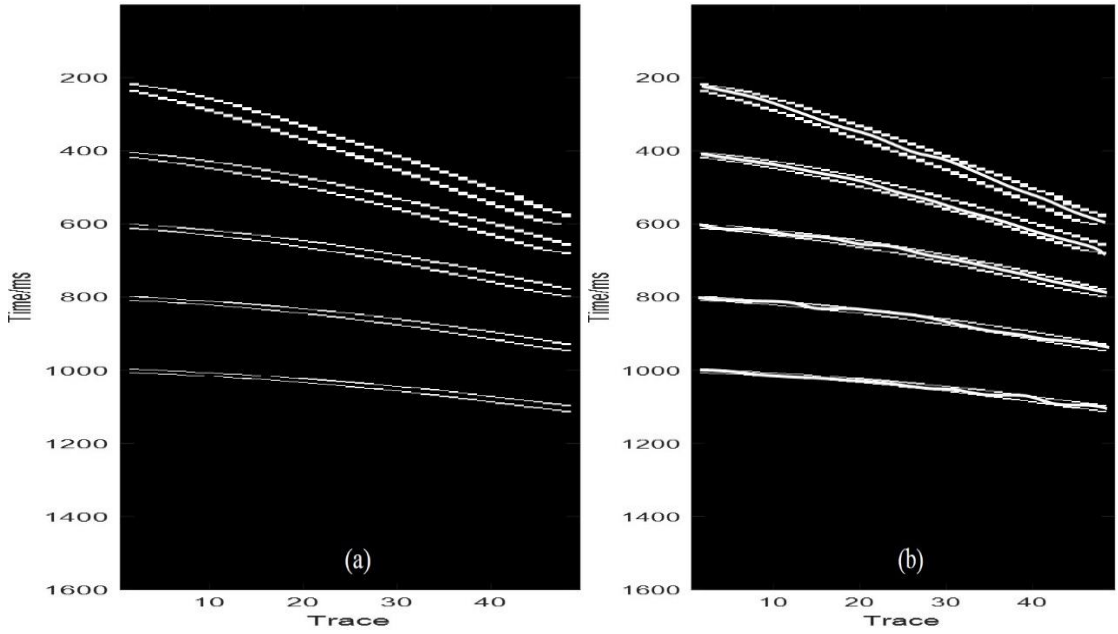

Fig. 9 (a) Result of edge detection and (b) auto event picking with Gaussian noise.

3.3 Data set 2: Real field reflection record

Real pre-stack common shot point (CSP) gather is shown in Fig. 10(a) and its corresponding IA section obtained by the wavelet transformation is shown in Fig. 10(b). The CSP gather has 595 traces, where the minimum offset is 90m, and the distance *dx* between two adjacent geophones is 10m. The corresponding SSPA section is shown in Fig. 11(a), and the detected edge of the SSPA section is given in Fig. 11(b). Fig. 11(a) shows that the slant stacked peak amplitude (SSPA) section has much clearer events and less interference compared to the IA section shown in Fig. 10(b). This is because the noise is compressed when stacking several traces along certain dip angles. Fig. 11(b) shows that the edge detection section is clear and accurate, which has good integrity and continuity. The edges detected from the SSPA section are closely corresponding to the associated events. From 500ms~1000ms, there are three events; and around 2000ms, there is one event. These events are illustrated by arrows in Fig. 11(b). Fig.12 is the

result of auto events picking by thresholding the gray scale intensity within the detected edges. Local continuous events and the corresponding travel-time are picked from the edge detection section. This method can reduce noise effectively, and overcomes the difficulty of picking successive events along wide offsets.

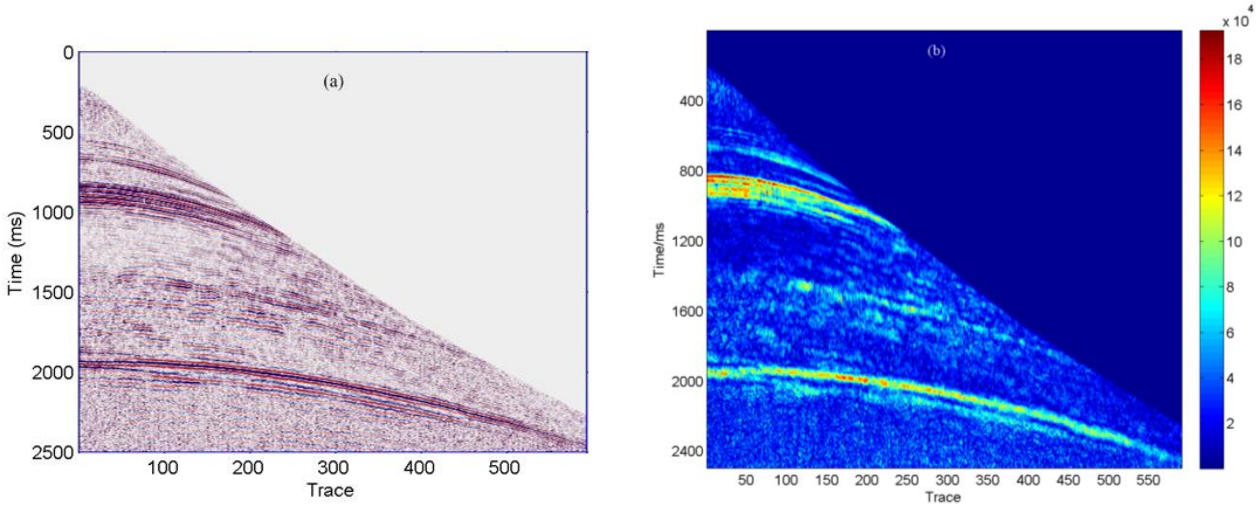

Fig. 10 (a) Real CSP gather； (b) IA section of CSP gather

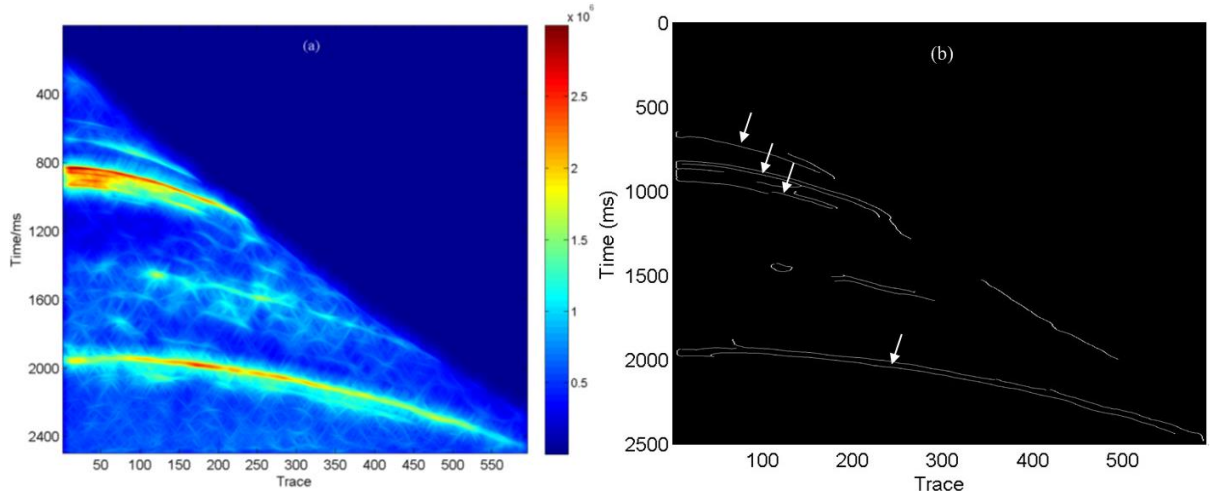

Fig.11 (a) The SSPA section; (b) The edge detection section

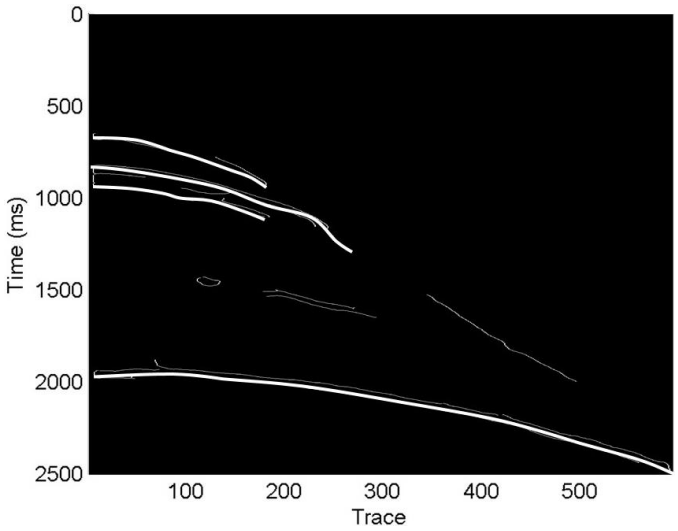

Fig. 12 The result of auto event picking using Canny operator

To further evaluate the performance of the proposed approach, another method named cross correlation is used for benchmarking. Fig.13(a) illustrates the principle of the cross correlation method, in which the maximum of cross correlation of two signals can be used to determine the delay time of the signals. This process can be repeated for other signals until the track of the events can all be obtained. This method needs to window the signals, as illustrated in Fig. 13(b), where the diagram shows the first ten traces moving along the hyperbole. Because the offset is too small, the hyperbole track of the events is not obvious. Fig.14 is the result of the events picking using cross correlation method, where noise interference can be clearly seen as highlighted by ovals. The picked events are discontinuous as indicated by arrows, and the operation is complex because of the windowing. By comparing Fig.12 and Fig.14, our proposed approach is more straightforward and effective in auto events picking, and the obtained result has clear and continuous edges but less noise than the ones from correlation based approach.

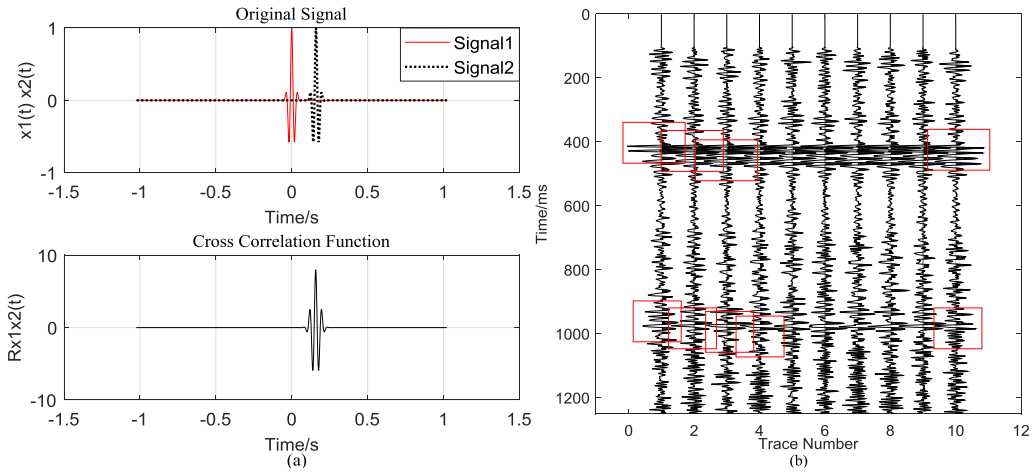

Fig.13 Illustration of the principle of the cross correlation method (a) and the diagram of the windowing (b).

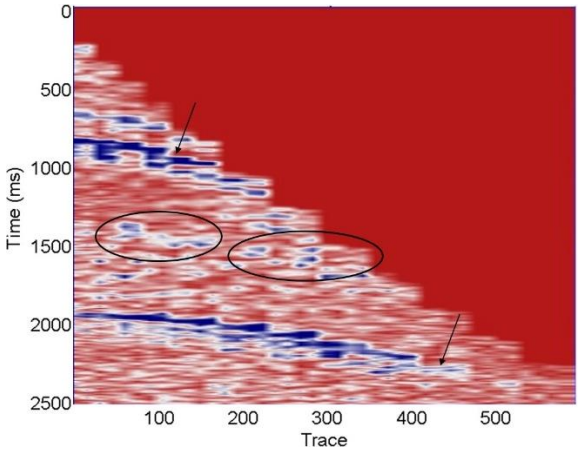

Fig.14 The result of the events picking using cross correlation method.

4. Conclusions

In this paper, a new local continuous events and travel-time picking method is proposed by detecting edges of the slant-stacked peak amplitude (SSPA) section. How to calculate the SSPA section without windowing and manual picking of seed points is detailed. The high resolution Radon transformation is discussed based on the instantaneous amplitude (IA) section. The optimal operator applied for edge detection based method is provided and benchmarked with conventional approaches. The flowchart of the proposed method is also summarized.

The proposed event picking method is effective and efficient, which overcomes the difficulty of picking continuous events along with a wide range of offsets. Our proposed method neither need to transform the seismic section to grayscale images nor sharpen the image. High accuracy and efficiency from the proposed method are shown in experiments with both synthetic pre-stack CMP gathers and real data. When the locations of the events are obtained, the travel-time can be picked directly from the records. The proposed method has great potential for seismic interpretation, where both the detected events and the picked travel-time can be used in waveform inversion, seismic attenuation estimation and gas reservoir characterization. Future work will focus on the interpolation method when the events are discontinuous as well as how to further improve the *SNR*.

Acknowledgment

This work is partially supported by the National Natural Science Foundation of China (41604113), National Nature Science Foundation Project of International Cooperation (41711530128), National Innovation and Entrepreneurship Training Program for College Students (201810705050), and Shanxi Hundred Talent Plan Project. We also thank Changqing oilfield for their field data.

References

Barnes A E, 1991. Instantaneous frequency and amplitude at the envelop peak of a constant-phase wavelet. Geophysics. 56(7): 1058-1060.

Barnes A E, 1993. Instantaneous spectral band-width and dominant frequency with applications to seismic reflection data. Geophysics. 58(3), 419-428.

Bian, Z., 2011. Study of Automatic Events Extraction on the Seismic Profiles Methods based on the QT Platform. Chengdu University of Technology.

Bondar, 1992. Seismic horizon detection using image processing algorithms. Geophysical Processing. 40(7):785-800.

Ding, W., Pan, G., et al., 2012. The research of interactive auto pickup of seismic events based on energy ratio and cross-correlation. Acta oceanologica Sinica. Vol.34, No.3.

Faraklioti, 2004. Horizon picking in 3D seismic data volumes. Machine Vision and Applications. 15(4):216-219.

Feng, Z.H., Liu, C., et al., 2011. A Method of Automatic First Arrival Extraction Based on One-Dimensional Slice of Cross-Fourth-Order Cumulants. Journal of Jilin University. 46(1):58-63.

Glinsky, M.E., 2001. Automatic event picking in prestack migrated gathers using aprobablistic neural network. Geophysics. 66(5):1488-1496.

Karbalaali, H., Javaherian, A., et al., 2017. Channel edge detection based on 2D compactly-supported shearlets: An application to a channelized seismic data in South Caspian Sea, 79th EAGE Conf. and Exhibition. 146:67-79.

Li, H., Liu, C., Tao, C., 2007. The Study of Application of Edge measuring Technique to the Detection of Phase Axis of the Seismic Section. Progress in Geophysics.

Li, X., 2014. Automatic seismic event pickup using edge measuring technique. Master thesis, Ocean University of China.

Li, Y., Yang, B., et al., 2005. An Algorithm of Chaotic Vibrator to Detect Weak Events in Seismic Prospecting Records. Chinese Journal of Geophysics. 48(6):1502–1508.

Lu, W., Mou, Y., 1998. Seismic event automatic tracking using self-organizing neural network. Geophysical Prospecting for Petroleum (in Chinese), 37(1): 77-83.

McComack, M.D., 1993. First-break refraction event picking and seismic data trace editing using neural network. Geophysics. 58(1):67.

Shen, C., Niu, B., Yu, Q., 2000. Implementing Radon Transform In Matlab. *Computing techniques for geophysical and geochemical exploration*, 22(4).

Spagnolini, U., 1991. Adaptive picking of refracted first arrivals. Geophy.Prosp. 39(3):293-312.

Tugnaait, H.K., 1991. On time delay estimation with unknown spatially correlated Guss noise using fourth-order cumulants and cross cumulants. IEEE Trans. Signal Processing. 39(6):1258-1267.

Wang, C., Gao, J., 2012. High-dimensional waveform inversion with cooperative coevolutionary differential evolution algorithm. IEEE Geoscience and Remote Sensing Letters, 9: 297-301.

Wang, Y., Sun, J., 2016. Study of formation boundary and dip attribute extraction based on edge detection technology. *Global Geology*, 109-116.

Woodham, C.A., 1995. 3-D Seismic Tracking with Probabilistic Data Association. Geophysics. 60(4):1088-1094.

Xiang, Y., Wang, F., et al., 2017. SAR-PC: Edge detection in SAR images via an advanced phase congruency model. Remote Sens. 9(3):209-.

Xiong, X., Guan, Y., et al., 2009. Extraction of Cophasal Axes on Seismic Sections based on the Edge Detection Method. Progress in Geophysics.

Xu, J., Wang, S., Zhao, T., 1990. Method on Auto Events Picking with Chain Match Algorithm. Geophysical Prospecting for Petroleum.

Yang, W., Cheney, K., 2011. The Seismic Reflection Cophasal Axes Checked by using Image Thin Algorithm. Complex Hydrocarbon Reservoirs.

Zhao, J., Ren, J.C., et al., 2018. Cognitive seismic data modelling based successive differential evolution algorithm for effective exploration of oil-gas reservoirs. Journal of Petroleum Science and Engineering, 171: 1159-1170.

Zhao, X., Li, Y., Yang, B., 2006. The Discussion to the Resilience Items in the Duffing Type System Used for Detecting Events. Chinese Journal of Geophysics.

Zhen, G.Y., 2013. The technology of seismic horizon automatic tracking. *Computing Technique for Geophysical and Geochemical Exploration*, 35(6).

Zhou, G., Hu, Z., 1991. AR Auto Tracking Events Method based on Seismic Profiles. ACTA Automatica Sinica.